Thank you for your thoughtful suggestions and comments.

Comments 1:

In my opinion, the lack of the integration of the coccoliths with coincident particles (quartz, clays, other calcite particles, including other coccoliths) represents a major caveat of the refinement of the decanting protocol. The Authors treat their assemblages as monospecific coccolith assemblages. For the large assemblages, which yielded 50% relative abundance of the target species, what is the effect of other calcite particles? If their composition change, would that change the settling velocity?

Reply: Good question. If our understanding is correct, we think your question can also be asked in another way: what's the behavior of particles in a multi-species or multi-particle type settling system?

Based on the work by Masliyah (1979), we know that when particle concentration is smaller than 10%, the collisions among particles don't have significant influence on sinking velocity. Hence, in a situation where there are several kinds of particles in the suspension, if the concentration is low enough, we can treat them as independence settlings. In our experiments, because the particles concentration were below 5%, we therefore think that varying composition of the suspension would have a negligible influence on the measured sinking velocities. This would be the case for a multi-species coccolith assemblage or one with different particle times, so long as total particle concentration remained low.

Comments 2:

More importantly, it is well known that clays are charged particles that are able to form aggregates ('flaks') in suspension and as such, these particles are prone to substantially influence the setting velocity. This issue is only briefly acknowledged by the 'hindered settling'. This is crucial for the application of the parameters in natural assemblages containing various concentrations (?nature) of clay minerals. Therefore I am of the opinion that this points need to be further discussed. Adding synthetic clay minerals in the assemblages would have been a sensitive means to address this criticism, although I am not advocating that the Authors should perform more experiments.

Reply: We emphasize that 'hindered settling ' is different to 'settling as aggregates'. As we mentioned in Lines 154-158 (Lines 134-141 in the former version), 'hindered settling' was caused by high concentration of suspension and collisions among particles. In the sample of ODP 807, there are aggregates in raw sediments even after 24 hours soaking in 0.2% ammonia. There is a protocol using benzalkonium chloride to disaggregate (Minoletti et al., 2008). In our pretreatments for this site, we discarded any large rapidly sinking aggregates that remained after soaking, before proceeding with settling steps. We now mention this in Lines 91-92. We acknowledge that, in this study, we have not tested the direct effect of disaggregated clays present in the solution on coccolith settling rates. However, as mentioned above, low concentrations should minimize these effects.

Comments 3:

It is not clear to me how many particles (coccoliths) were actually counted, nor if replicated measurements have been conducted? Also, it would be good to explain the 'drop technique' used in this study.

Reply: Thank you for pointing this out. In most experiments, more than 300 (usually around 500) coccoliths were counted. For *H. carteri*, we counted more than 100 FOVs and about 100 specimens because the number of *H. carteri* is much smaller than other coccolith even after pretreatments. We have added this statement in the new version (Lines 113-119).

Comments 4:

It is not clear from reading the text why Helicosphaera carteri escapes the settling velocity equation derived for other taxa (L203-205).

Reply: Thanks for pointing out that this needs clarification. We didn't use *H. carteri* in the regression because of its specific shape, which is quite different to the other species studied. This was explained it in Lines 224-233 (Lines 203-205 in the former version): the ellipticity of *H. carteri* (~0.6) is

significant lower than other coccolith (among 0.8-0.9), therefore its settling behavior differs from other species. This is also illustrated in Figure 6d and Figure C3. We have reorganized this part to make it clearer.

Comments 5:
Why is the potential of centrifuging not discussed at all - except a brief mention L47?
Reply: This is a good point and a question that we are currently working on. To data, we have calculated the movement of coccoliths in a centrifuge machine and tried to use centrifuging instead of gravity settling. The centrifuging method works well for small coccolith such as *F. profunda* and *E. huxleyi*. However, the uncertainty will become larger when we try to separate large coccolith such as *C. pelagicus*. We are still working on improving the centrifuging method, which would be the subject of a future publication and we would prefer to focus on sinking velocity measurements under gravity in this study.

Comments 6:
Figure 1 should include the array of sizes of the various coccoliths presented.
Reply: Thank you for your suggestion. We have listed mean sizes and standard deviations of size in Table 2. Since Figure 1 showed the evolutionary ranges timing of different coccolithophores and the coccoliths' size for each species varied in geological time, we think plotting the size data in our sample with fixed values on Figure 1 could be misleading.

Comments 7:
Figure 2 is not really convincing given the number of coccoliths in the field of view.
Reply: We have redrawn Figure 2 and replaced these photos by a schematic drawing. See the new version Figure 2.

Comments 8:
That Pseudoemiliania lacunosa and Umbilicosphaera sibogae are impossible to differentiate is premature here, and should be discussed later in the manuscript.
Reply: We have changed this sentence as '*Pseudoemiliania lacunosa* and *Umbilicosphaera sibogae* were measured together' and we have modified the former 'Conclusions' part as 'Suggestions for coccolith settling velocity estimations and separations' and you can find an explanation in Lines 277-279.

Comments 9:
L143 "in ammonia at 20_C" – I guess you mean in deionized water neutralized by addition of ammonia?
Reply: Yes. We have changed this sentence as 'in 0.2% ammonia at 20℃'.

Comments 10:
L348 : Publication date is 2009. L415 Pseudoemiliania lacunose is mispelt. L420 Calcidiscus leptoporus is mispelt. (Many other taxa are misspelt throughout the text and captions).
Reply: We apologize for the spelling mistakes. We have done double checks in this new version. We have changed publication data in Line 34, 88 and 411.

References:
Masliyah, Jacob H. "Hindered settling in a multi-species particle system." Chemical Engineering Science 34.9 (1979): 1166-1168.
Minoletti, Fabrice, Michaël Hermoso, and Vincent Gressier. "Separation of sedimentary micron-sized particles for palaeoceanography and calcareous nannoplankton biogeochemistry." Nature protocols 4.1 (2008): 14.

A refinement of coccolith separation methods: Measuring the sinking characters of coccoliths

Hongrui Zhang[1,2], Heather Stoll[2], Clara Bolton[3], Xiaobo Jin[1], Chuanlian Liu[1]

[1] State Key Laboratory of Marine Geology, Tongji University, Shanghai, 200092, China

[2] Geological Institute, Department of Earth Science, Sonneggstrasse 5, ETH, 8092, Zürich, Switzerland

[3] Aix-Marseille Univ, CNRS, IRD, Coll de France, CEREGE, Aix en Provence, France.

Correspondence to: Chuanlian Liu (liucl@tongji.edu.cn)

Abstract. ~~The~~ Quantification sinking velocities of individual coccoliths ~~are relevant~~will contribute to ~~for export of their CaCO3 from the surface ocean, and for~~ optimizing laboratory methods ~~to~~ for separat~~ing~~e coccoliths of different sizes and species for geochemical analysis. ~~In the laboratory, t~~The repeat settling/decanting method was the earliest method proposed to separate coccolith~~s~~ from sediments ~~for geochemical analyses~~, and is still widely used. However, in the absence of estimates of settling velocity for non-spherical coccoliths, previous implementations have depended mainly on time consuming empirical method development by trial and error. In this study, the sinking velocities of coccoliths belonging to different species were carefully measured in a series of settling experiments for the first time. Settling velocities of modern coccoliths range from 0.154 to 10.67 cm h^{-1}. We found that a quadratic relationship between coccolith length and sinking velocity fits well and coccolith sinking velocity can be estimated by measuring the coccolith length and using the length-velocity factor, k_{sv}. We found a negligible difference in sinking velocities measured in different vessels. However, an appropriate choice of vessel must be made to avoid 'hindered settling' in coccolith separations. The experimental data and theoretical calculations presented here ~~will~~ support and improve the repeat settling/decanting method.

1. Introduction

Coccolithophores are some of the most important phytoplankton in the ocean. They can secrete calcareous plates called coccoliths, which contribute significantly to discrete particulate inorganic carbon in the euphotic zone and to $CaCO_3$ fluxes to the deep ocean (e.g., Young and Ziveri, 2000; Sprengel et al., 2002) , andCoccolith morphyology, geochemisity and fossile assemblage composition can reflect record paleoenvironmental changes (e.g., Beaufort et al., 1997; Stoll et al., 2002; Zhang et al., 2016). However, the use of coccolith geochemical analyses in paleoenvironmental reconstructions is was so far hindered by the difficulty of isolating coccolith compared with foraminifera. Two main methods have been developed to concentrate near-monospecific assemblages of coccoliths from bulk sediments: one is the method based on a decanting technique (Paull and Thierstein, 1987; Stoll and Ziveri, 2002) and the other is that based on microfiltration (Minoletti et al., 20082009). The improvement of separation techniques offered a new perspective to study the Earth's history (e.g. Stoll, 2005; Beltran et al., 2007; Bolton and Stoll, 2013; Rousselle et al., 2013). Moreover, the development of coccolith oxygen and carbon isotope studies in culture in recent years (e.g. Ziveri et al., 2003; Rickaby et al., 2010; Hermoso et al., 2016; McClelland et al., 2017) has provided an improved mechanistic understanding of coccolith isotope data and therefore stimulated the need for more purified coccolith fraction samples from the fossil record.

Both decanting and microfiltering are widely used methods for coccolith separation. The mMicrofiltering method separates coccoliths with polycarbonate mirco-filter membrane relies heavily on the specifications of micro filter membrane (such aswith pore sizes of 2μm, 3μm, 5μm and 8μm, 10μm and 12μm pore size). and This method is highly effective in the larger size ranges, but is very time consuming in sediments with a high proportion of very small (<5μm) coccoliths (which tends to be the case in natural populations). It is also impossible to separate coccoliths with similar lengths by microfiltration, such as *Florisphaera profunda* and *Emiliania huxleyi* (Hermoso et al., 2015). Decanting, on the other hand, is highly effective for the small-sized coccoliths, because their slow settling times permit a greater ability to separate different sizes. Consequently, in some studies, a combination of the micro filtering and sinking or centrifugation method were applied for coccolith separation (Stoll, 2005; Bolton et al., 2012; Hermoso et al., 2015). The repeated

sinking/decanting method, first employed by (Edwards, 1963; Paull and Thierstein, 1987) follows the simple principle formalized by Stokes' Law for spherical particles: particles of larger size settle more quickly because they have a higher ratio of volume and mass (accelerating sinking) to sectional area (resistance retarding sinking).   However, the sinking velocities of coccoliths with complex shape are difficult to calculate and have not been quantified in previous studies. Consequently, the repeated decanting method has generally used settling times based on empirical trial and error.

In this the current study, we present a novel and rigorous estimation of the sinking velocity for 16 species of modern and Cenozoic coccoliths, carefully measured in 0.2% ammonia at 20℃. With this new dataset, we explore how to estimate the sinking velocity of coccoliths based on theirby shape and length, which allows our estimations to be generalized for other species, and for situations where the mean thickness length of coccoliths of a given species was different from that of our study. These generalizations, together with our results on sinking velocities of one coccolith species (*Gephyrocapsa oceanica*) in different vessels, should allow a significant improvement in efficiency of future protocols for separation of coccoliths by repeated decanting.

2. Materials and methods

2.1 Sample selections

We measured the sinking velocity of 16 different species of coccoliths,– isolated from eight deep-sea sediment samples from the Pacific and Atlantic Oceans (Figure 1, Table A1). Sample were principally of Quaternary age but – includinginclude two Neogene/Paleogene samples (Figure 1). In general, nNumbers of small coccoliths, including *E. huxleyi*, *Gephyrocapsa* spp and *Reticulofenestra* spp. are about an order of magnitude greater than that of larger coccoliths. However, the larger coccoliths' contributions to carbonate can be as high as 50% (Baumann, 2004; Jin et al., 2016). Moreover, both small coccoliths and large coccoliths are useful in geochemical analyses (Ziveri et al., 2003; Rickaby et al., 2010; Candelier et al., 2013; Bolton et al., 2012, 2016; Bolton and Stoll, 2013). Therefore, both small and large coccoliths were studied in this research. The coccoliths were isolated from eight samples from the Pacific and Atlantic Oceans (more location information are in Figure 1 and Table A1; the pictures of studied coccolith can be found in Appendix B). All Pictures of the studied coccolith are shown in Appendix B, and all classifications of coccolith

3

80   follow Nannotax3 except *Reticulofenestra* spp. (Figure C2 in Appendix C).

81   **2.2 Experiment designs**

82   **2.2.1 Sample pretreatments**

83   The sinking velocity measurement depends on absolute abundance estimation (more details in 2.2.2).

84   However, on microscope slides, larger coccoliths and foraminifer fragments may cover smaller

85   coccoliths, reducing the accuracy of coccolith absolute numbers. Thus, before sinking experiments

86   were carried out, raw sediments were pretreated to purify the target coccoliths to reduce errors in

87   coccolith counting. The raw sediments were disaggregated in 0.2% ammonia and sieved through a

88   63 μm sieve and then treated by sinking method or filtering method (Bolton et al., 2012; Minoletti

89   et al., ~~2008~~2009) to concentrate the target species up to at least more than 50% of the total

90   assemblage~~s~~ (for Noëlaerhabdaceae coccoliths, a percentage more than 90% can be easily achieved).

91   In one sample with aggregation (ODP 807), we did a rapid settling (30 min, 2 cm) to eliminate

92   aggregates. Most of the species were measured individually in settling experiments, except ~~the~~ for

93   *Pseudoemiliania lacunosa* and *Umbilicosphaera sibogae*, which ~~cannot be separated from each~~

94   ~~other~~were measured together.

95   **2.2.2 Measuring the sinking speeds of coccoliths**

96   We are not aware of any prior direct determination of the sinking velocity of individual coccoliths,

97   although the sinking velocities of live coccolithophores and other marine ~~algae~~ algal cells have been

98   successfully measured by the 'FlowCAM' method (Bach et al., 2012) or a similar photography

99   technique (e.g. Miklasz and Denny, 2010). Here we introduce a simple method to measure the

100 particle sinking speeds without special equipment.

1.   After pretreatment, the coccolith suspensions were gently shaken and then moved into comparison tubes which were vertically mounted on tube shelves. We set the timer going and let the suspension settle for a specified period of time, marked as sinking time or settling duration (T).

2.   Thereafter, we removed the upper 15 ml supernatant into a 50 ml centrifuge tube with a 10 ml pipette. This operation ~~should be~~was performed slowly and gently to avoid drawing lower suspensions upward. The absolute counting of cocolith was achieved by using the 'drop technique' to make quantitative microscope sides (Koch and Young, 2007; Bordiga

4

109   et al., 2015). 0.3 ml mixed suspension was extracted and pipettes onto a glass cover and

110   dry the slider on a hotplate;

111   3.   The lower suspension was than to homogenized and another slider was prepare as described

112   above;

113   4.   The number of coccoliths in the upper and lower suspensions were carefully counted by

114   the 'drop technique' on microscope at ×1250 magnification and the number of coccoliths

115   and fields of view (FOV) were recorded for further calculations. , which is a quick method

116   to determine absolute abundance of coccoliths (Koch and Young, 2007; Bordiga et al.,

117   2015). More than 300 specimens were counted for most of the measurements. For the

118   *Helicosphaera carteri* measurements, more than 100 FOV were checked and about 100

119   specimens were counted.

120   To calculate the sinking velocities of coccoliths, we define a parameter named the separation ratio

121   (R), which represents the percentage of removed coccoliths in one separation by pumping out the

122   upper suspension. This parameter is important and will be repeatedly mentioned in the following

123   part. R was measured using the following equation (more details about derivation can be found in

124   Appendix D):

125
$$R = \frac{\frac{N_1}{n_1} \times V_1 V_1}{\frac{N_1}{n_1} \times V_1 V_1 + \frac{N_2}{n_2} \times V_2 V_2} \tag{2-1}$$

126   where N_1 and N_2 are numbers of coccoliths counted in upper and lower suspension slides,

127   respectively; n_1 and n_2 are the number of fields of view (FOV) counted. V_1 and V_2 are the volume

128   of the settling vessel defined by the settling distance, as shown in Figure 2.

129   The separation ratio, R, also has a relationship with sinking time, T (Appendix D):

130
$$R = \frac{V_1 - \frac{V_1}{D} \times sv \times T}{V_1 + V_2} \tag{2-2}$$

131   where V_1, V_2 and D are shape parameters shown in Figure 2; and sv v is the average sinking velocity

132   of measured coccoliths. If we plot R against T, the slope of line has a relationship with sv. Hence

133   Then liner regressions between R and T were processed with MATLAB to calculate the sv (details

134   about error analyses can be found in Appendix E).

135   There are still two issues to be explained. The first one Firstly, is to eliminate the shape differences

136   among vessels, all separation ratios have been transferred to calibrated separation ratios (R_{cal}), which

137   means the separation ratio measured in a standard vessel with V_1=15 ml, V_2=10 ml and D=6 cm

138 (more details about transformation from R to R_{cal} can be found in Appendix D). The other one is

139 thatSecondly, we treated the average sinking velocities as the sinking velocities of the coccoliths

140 with the average length. This approximation has been proved reasonable in Appendix D.

2.2.3 Detecting the potential influence of vessels

142 Seven commonly used vessels were selected to detect the potential influence of vessels (Figure 3).

143 Two of them are made of plastics (No.2 and No.3 in Figure 3) and all others are pyrex glass vessels.

144 About 500 mg of sediment from the core KX21-2 were pretreated as described in 2.2.1 and

145 suspended in about 500 ml ammonia. After that, settling experiments were performed as described

146 in 2.2.2 using different vessels. In these experiments, only the dominant species, *G. oceanica*, was

147 measured.

2.2.4 Other factors influencing the sinking velocity

149 Temperature can change the density and viscosity of liquid. Generally speaking, the higher the

150 temperature is, the lower the density and viscosity will become and the faster pellets will sink. Take

151 water for instance, if the temperature increases from 15 to 30℃, the particle sinking velocity will

152 increase by ~43% (Table 1). All sinking velocities measured or discussed in the following sections

153 were velocities at 20℃ to minimize the influence of temperature.

154 The calibration of sinking velocity in high concentration suspension has been calculated by

155 Richardson and Zaki (1954)

$$sv = sv_0(1 - \alpha_s)^{2.7} \tag{2-3}$$

157 where the α_s is the solids volume fraction. Based on equation 2-3, the higher the suspension

158 concentration is, the slower the sinking velocity will be. That is so called 'hindered settling'. When

159 the α_s=0.2%, the reduction of sinking velocity owing to hindered settling is negligible cannot be

160 neglectable (sv/sv$_0$ equals 99.46%). Hence, in this study all suspensions have solid volume fractions

161 lower than 0.2% to avoid notable reductions of coccolith sinking velocities.

3. Results and Discussions

3.1 Influence of vessels

164 The sinking velocities of *G. oceanica* in the core KX21-2 in 0.2% ammonia at 20℃ measured in

165 different vessels vary from 0.99 to 1.23 cm h^{-1}. The lowest value occurred in the 100 ml centrifuge

166 tube and the highest sinking velocity was measured in the 50 ml centrifuge tube experiments. The

167 correlations between sinking velocities and different vessel parameters are quite low: r=0.13 for the

168 vessel inner diameter, r=0.0005 for the sinking distance and r=0.051 for the upper volume and total

169 volume ratio ($V_1/(V_1+V_2)$)). The dissipation of energy by friction between the moving fluid and the

170 walls can cause a reduction of sinking speed (wall effect). A significant wall effect will be detected

171 when a particle is settling in a vessel which with a diameter that is smaller than the particle size by

172 two orders of magnitude (Barnea and Mizarchi, 1973). The length of coccoliths is on the micron

173 scales, so the diameters of vessel used in laboratory are about more than three four orders of

174 magnitude larger than coccoliths. Moreover, our results show that the difference between vessel

175 materials, glass and plastics, can also be ignored (Figure 4). Hence, we suggest that vessel type

176 almost has no significant influence on sinking velocity of coccoliths.

177 However, our experiments were premised on the basis that the concentration of suspension was

178 equal among different vessels. This means that large vessels can treat more sediment at one time but

179 if we choose a larger vessel, more suspensions should be pumped and it often costs more time in

180 sinking (often due to longer sinking distance). Assuming that the sediment is composed of 50%

181 calcite (with density of 2.7 g cm^{-3}) and 50% clay (about 1.7 g cm^{-3}), the largest amount of sediment

182 that can be used without significant reduction of the sinking velocity (5%) is about 400 mg in 100

183 ml suspension (this calculation is based on equation 2-3). However, becausethe sediments

184 accumulating accumulate in the lower suspension, the particle concentration can be more than 4

185 times higher than in the initial homogenous concentration. This phenomenon will be more

186 significant for a vessel with a narrow bottom, such as centrifuge tubes. To avoid this, we recommend

187 using about 100 mg dry sediment should be suspended in at least 100 ml suspension to avoid

188 'hindered settling'. If more sediment is necessary for geochemistry analyses, then a larger vessel

189 should be selected to separate enough sample in at one time.

190 **3.2 Sinking velocities at 20℃ in 0.2% ammonia**

191 We measured the separation ratios of different coccoliths in comparison tubes at 20℃ in 0.2%

192 ammonia (Figure 5). The sinking velocities of coccoliths were then calculated by linear fitting of

193 separation ratios and settling durations. The sinking velocities of studied coccoliths vary by one two

194 orders of magnitude from 0.154 cm h^{-1} to 10.67 cm h^{-1} (Table 2). The highest sinking velocity was

195 found in the measurement of *Coccolithus pelagicus* and the lowest velocity was found for *F.*

196 *profunda*. The average sinking speeds of coccoliths is about 10-50% of the terminal sinking

197 velocities of calcite spheres calculated by Stokes' Law (Figure 6c). These ratios are comparable ~~with~~

198 ~~the~~to the oval objects (e.g. seeds) data from Xie and Zhang (2001) and smaller than steel ellipsoids

199 ~~those~~ data from McNown and Malaika (1950). The sinking velocities of coccoliths measured in our

200 experiment are about 2-3 orders of magnitude smaller than values from sediment traps of 143-243

201 m d^{-1} (595~1012 cm h^{-1}) in the North Atlantic (Ziveri et al., 2000 and Stoll et al., 2007), ~~confirming~~

202 suggesting ~~the fact~~ that the coccoliths sinking out of the euphotic layer are mainly in the form of

203 sinking aggregates rather than individual coccoliths.

3.3 Estimating the sinking velocities

205 Generally speaking, the sinking velocities of coccoliths increase with ~~the~~ distal shield length (Figure

206 5a), as expected from the increase in volume to sectional area for a given geometry as length

207 increases. Our data implies that the sinking velocity has a power function relationship with distal

208 shield length.

209 We propose that the sinking velocity of coccoliths might have a quadratic relationship with distal

210 shield length as described by Stokes' Law (Figure 6a). If we use data for all species except

211 ~~*Helicosphaera*~~ *H. carteri* ~~,~~(the reason can be found in the following discussion), the sinking

212 velocities can be described by the following equation:

$$v = 0.0982 \,(\pm 0.001){*}\, \phi^2 \tag{3-1}$$

214 Based on this quadratic regression, we derive a shape-velocity factor (k$_{sv}$) that relates settling

215 velocity to coccolith length.

$$v = k_{sv}{*}\, \phi^2 \tag{3-2}$$

217 Furthermore, this factor is analogous to the shape-mass factor, 'k$_s$' used to relate coccolith mass to

218 coccolith length (Young and Ziveri, 2000). The length and shape-velocity factor of coccoliths can

219 be used to predict most of the sinking velocity variations, however, variations may also arise due to

220 changes in coccolith mass and thickness, for a given length, and due to the hydrodynamics of

221 particular shapes. We noticed that the smaller coccolith *G. caribbeanica* has a greater sinking

222 velocity than the larger coccolith, *G. oceanica*. We suggest that this was caused by greater mass per

223 length (or greater average thickness) in the case of *G. caribbeanica* and this may be due to the closed

8

224 central area while *G. oceanica* has an open central area. Another example is *H. carteri*, ~~its~~ which

225 ~~lower~~smaller sinking velocity of which can be explained by the unique structure of *H. carteri*

226 coccolith ~~:~~. Firstly, the broad edge of *H. carteri* can increase the drag force significantly. ~~and *H.*~~

227 ~~*carteri* has the largest ellipticity (major axis length and minor axis length ratio) among the measured~~

228 ~~coccoliths, which means the mass of *H. carteri* is smaller than other species of coccoliths with~~

229 ~~similar lengths (Figure 6d and Figure C3).~~ Moreover, most of the measured coccoliths have a

230 ellipticity (major axis length and minor axis length ratio) larger than 0.8, while the ellipticity of *H.*

231 *carteri* is around 0.6, which means the mass of *H. carteri* is smaller than other species of coccoliths

232 with similar lengths (Figure 6d and Figure C3). That is also the reason *H. carteri* was excluded from

233 the general regression in equation 3-1. In the case of partial dissolution, the well-preserved

234 *Cyclicargolithus floridanus* may have higher mass than dissolved (or disarticulated) *Cy. floridanus*,

235 and therefore a slightly higher shape-velocity factor.

236 **4. ~~Conclusions~~Suggestions for coccolith velocity estimations and separations**

237 To improve coccolith separation by settling methods, we measured sinking velocities of different

238 coccoliths by gravity. Sinking velocities in this study varied from 0.154 to 10.61 cm h^{-1}, about 10%

239 to 50% of those of calcite spheres with same diameter. The shape of different vessels had little

240 impact on the sinking velocity. But we should consider the volume of vessels to avoid 'hindered

241 settling'. The sinking velocities are mainly controlled by the shape of coccolith, including the distal

242 shield length, the size of central area, and the ellipticity of coccoliths. Besides the shape of coccoliths,

243 temperature is also crucial to the coccolith separations because of the dependence of sinking

244 velocities on temperature. Length-velocity factors were proposed to estimate coccoliths sinking

245 velocities, so coccolith ~~sinking speeds in different samples can be easily estimated~~separation can be

246 achieved by following steps:

247   1) Measure the ~~mean~~ length of coccoliths in your target assemblage under the

248   microscope and regress the length distribution by the assumption of normal distribution

249   (details are in Appendix C);

250   2) Estimate sinking velocities for each important species. For species which sinking

251   speed has been directly measured, we can use the length-velocity factor directly (v=k$_v$*

252   ϕ^2). For unmeasured species, we can choose the length-velocity factor of coccoliths

253 with similar morphology in this study or use the general length-velocity formula

254 $(v=0.098(\pm 0.001)* \phi^2)$;

255 3) Calculate the separation time for main species. For example, in KX21-2 there are three

256 main coccoliths, *F. prounda*, *G. oceanica* and *Ca. leptoporus* and we wish to separate

257 *G. oceanica* out from the bulk sediment. Calculate each cococliths' sinking velocity

258 distributions as described in Step 2 above. As shown in Figure 7, a sinking velocity

259 intermediate between *F. profunda* (with a length 2σ larger than average, marked as +2σ)

260 and G. oceanica (with a length 2σ smaller than average, marked as -2σ) optimal to

261 separate them, would be 0.6 cm h^{-1}. Similarly, we can chose speed thresholds 1.85 cm

262 h^{-1} to separate *G. oceanica* from *Ca. leptoporus*. If we settle in a 50 ml centrifuge tube

263 with a sinking distance, D, equal to 5.84 cm, the sinking time for separating *F. profunda*

264 should be T=5.84/0.6=9.73 h. Similarly, we can calculate the time for separating *G.*

265 *oceania* by T=5.84/1.85=3.16 h;

266 4) Homogenize the sediment suspension and let coccoliths settling as the period

267 calculated in Step 3. After that, pump out the upper part of suspension. In the upper

268 part, we have exclusively the smaller of the main coccoliths. However, column will

269 still contain some smaller ones. So this step (settling and pumping) should be repeated

270 until the lower part no longer has significant contribution from the smaller coccoliths.

271 This step has been well described in pervious studies and more details can be found in

272 Stoll and Ziveri (2002) and Bolton et al. (2012).

273 We find, i~~If~~ we use the general formula, ~~it should be noted that~~ a closed central area coccolith will

274 sink faster than prediction (for *G. caribbeanica* and small *Ca. leptoporus* will settle ~40% faster)

275 and coccoliths with greater ellipticity can settle much slower (for *H. carteri* will settle as 30% of

276 the predicted sinking velocity for coccolith with similar length). Moreover, the sinking method

277 cannot separate every species of coccoliths perfectly. As mentioned in Section 2.2.1, *P. lacunosa*

278 and *U. sibogae* cannot easily be separated from each other because they have similar sinking

279 velocities. Nevertheless, this study provides the first direct estimation of coccolith settling velocities,

280 which should simplify implementation of future methods to separate coccoliths by settling time.

281

287 **Table 1.** The influence of temperature on sinking velocity. Density data is from Kell (1975) and

288 viscosity data is from Joseph et al. (1978).

T (℃)	ρ (g cm⁻³)	η (mPa s)	$\mathrm{\cancel{SV}\underline{v}_T} : \mathrm{\cancel{SV}\underline{v}_{T=20}}$
15	0.9991	1.1447	0.8804
20	0.9982	1.0087	1
25	0.9970	0.8949	1.1279
30	0.9956	0.8000	1.2627

289 **Table 2.** The sinking velocity and shape-velocity factor of different coccolith species: ϕ means the

290 distal shield length of coccolith and St ϕ is the standard deviation of distal shield length; sv represents

291 the sinking velocity; $\cancel{sv}\underline{v}$ (95%-) and $\cancel{sv}\underline{v}$ (95%+) represent the lower and higher limit of 95%

292 confidence level, respectively. 'k_{sv}' represents the length-sinking velocity factor. The short name of

293 coccolith can be found in the caption of Figure 4. The details of coccoliths length distribution are in

294 Appendix C.

Species	abb.	ϕ (µm)	St ϕ (µm)	sinking velocity (cm h⁻¹)	$\cancel{sv}\underline{v}$ (95% -)	$\cancel{sv}\underline{v}$ (95% +)	k_{sv}
F. profunda	Fp-WP	1.508	0.557	0.158	0.010	0.011	0.070
F. profunda	Fp-SCS	1.786	0.641	0.154	0.051	0.052	0.048
small *Reticulofenestra*	Ret (<4um)	2.454	0.509	0.848	0.354	0.416	0.141
E. huxleyi	Emi	2.512	0.469	0.853	0.054	0.064	0.135
Gephyocapsa spp.	G spp	2.755	0.502	0.752	0.125	0.147	0.099
G. caribbeanica	Gcar	3.312	0.352	1.873	0.174	0.192	0.171
U. sibogae	Umb	4.060	0.500	1.268	0.416	0.441	0.077
G. oceanica	Geo	4.187	0.517	1.170	0.155	0.178	0.067
P. lacunosa	Pla	4.350	0.617	1.171	0.337	0.338	0.062
Small *Ca. leptoporus*	Cal small	4.605	0.629	3.351	0.172	0.199	0.158
large *Reticulofenestra*	Ret(>4um)	4.988	0.605	2.379	0.534	0.641	0.096
Cy. floridanus	Cyf	5.805	0.963	4.174	0.320	0.336	0.124
(dissolved) *Cy. floridanus*	Cyf -d	6.134	0.727	4.508	0.352	0.417	0.120
Large *Ca. leptoporus*	Cal large	6.370	0.931	3.737	1.053	1.336	0.092
H. carteri	Hel	8.936	0.994	2.541	1.740	2.440	0.032
Co. pelagicus	Cpl	10.640	1.175	10.610	0.950	1.235	0.094

295

296   **Figure 1**. Temporal and spatial distribution of samples. (a) The evolution of studied coccoliths: first

297   occurrence and last occurrence data are from Nannotax3

298   (http://www.mikrotax.org/Nannotax3/index.html). The blue bars represent ranges of first occurrence

299   and the green bars represent ranges of last occurrence. The blue diamonds represent samples used in

300   this study. (b) Spatial distribution of samples. 1304 means IODP U1304, 3428 means MD12-3428cq,

301   1433 and 1435 means IODP U1433 and U1435, respectively. 807 means ODP 807 and 21-2 means

302   KX21-2.

303

304
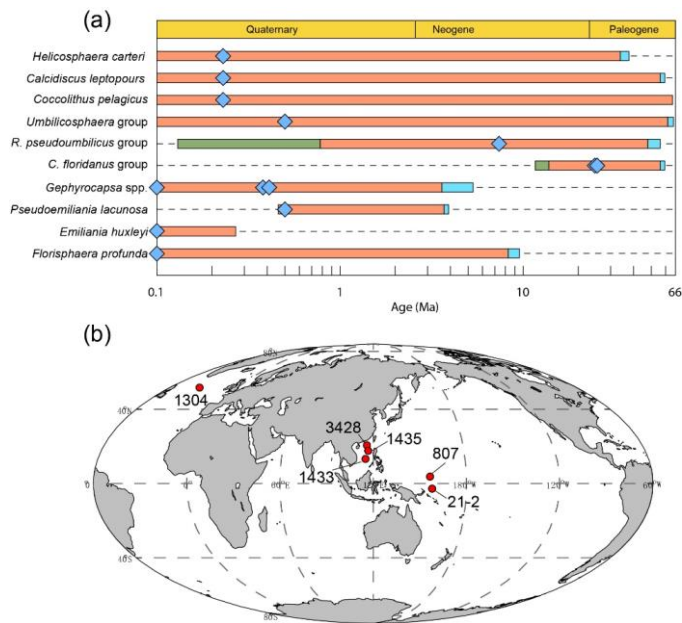
Figure 2. Schematic of settling experiments. ~~The pictures were taken after *Coccolithus pelagicus*~~ ~~sinking experiments with T=0 and T=30 min.~~ V_1 and V_2 are the volumes of the upper and lower cylinders, D is the settled distance. The numbers in circles are same as the number of Steps described in Section 2.2.1.

310
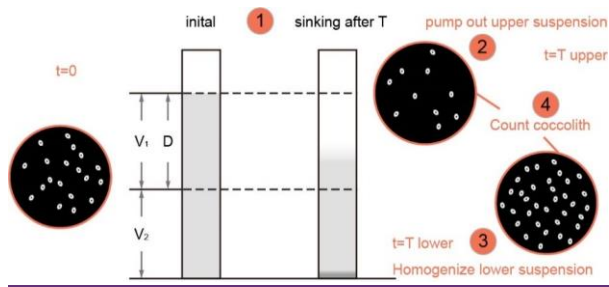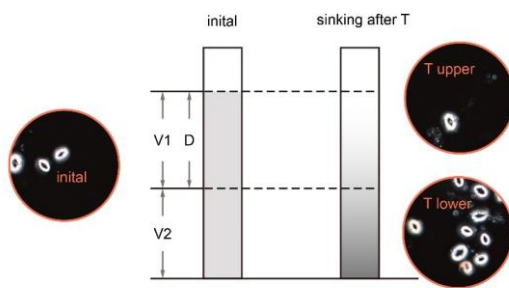
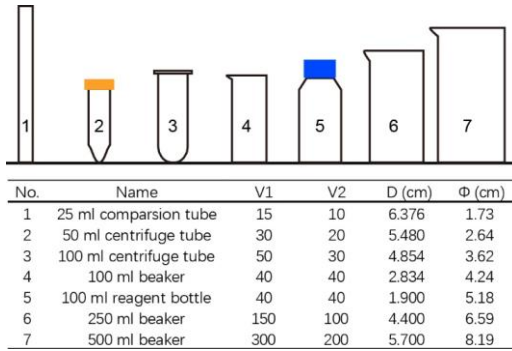311 **Figure 3.** The shape parameters of vessels. V_1 and V_2 means the volume of upper suspension and lower

312 suspension, respectively. D means sinking distance. Φ means average inner diameter which is

313 calculated by $2*(V_1/(\pi D^2))^{1/2}$.

| No.	Name	V1	V2	D (cm)	Φ (cm)
1	25 ml comparsion tube	15	10	6.376	1.73
2	50 ml centrifuge tube	30	20	5.480	2.64
3	100 ml centrifuge tube	50	30	4.854	3.62
4	100 ml beaker	40	40	2.834	4.24
5	100 ml reagent bottle	40	40	1.900	5.18
6	250 ml beaker	150	100	4.400	6.59
7	500 ml beaker	300	200	5.700	8.19

314
315

316 **Figure 4.** Sinking velocities of *G. oceanica* in the core KX-21-2 measured in different vessels. (a) The

317 calibrated separation ratios measured in different vessels. Error bars show 95% confidence level of

318 calibrated separation ratio. (b-d) The relationship between sinking velocity and different vessel shape

319 parameters. Error bars represent 95% confidence level of sinking velocity in each vessel and the shade

320 area represents 95% confidence level of sinking velocity considering all data points.
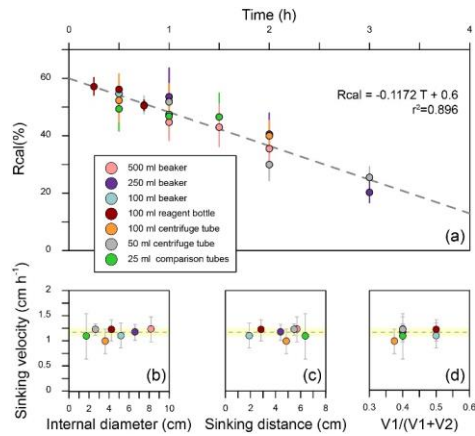
321

322 **Figure 5.** The calculated separation ratio (Rcal) vs sinking duration. Fp-WP means *F. profunda* in the

323 West Pacific. Fp-SCS means *F. profunda* in the South China Sea. Emi means *E. huxleyi*. Gspp means

324 small *Geophyocapsa*. Geo means *G. oceanica*. Gcarb means *G. caribbeanica*. Ret<4 means small

325 *Reticulofenestra*. Ret>4 means large *Reticuloenestra*. Cyf means *Cyclicargolithus floridanus*. Cy-d

326 means dissolved *Cy. floridanus*. Umb means *U. sibogae*. Pla means *Pseudoemiliania*

327 *lacunoselacunosa*. Hel means *Helicosphaera H. carteri*. Cal large means larger *Calicidiscus*

328 *leptoporus*. Cal small means small *Ca. leptoporus*. Cpl means *Co. pelagicus*.

329
330
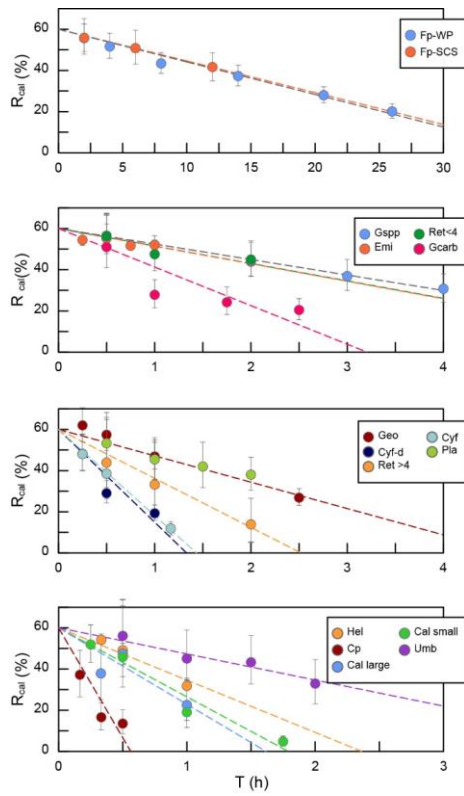
Figure 6. Coccolith sinking velocities and coccolith shape factors. (a-b) Sinking velocities and mean distal shield length. The horizontal error bars represent one standard deviation of coccolith length and the vertical ones represent 95% confidence level of measured sinking velocities. The blue, green and red lines represent sinking velocity of calcite sphere objects, coccolith sinking velocities estimated by Bolton et al. (2012) and this study, respectively. (c) The ratio of measured speed and speed calculated by Stokes' Law. (d) Coccolith short axis length (SAL) and long axis length (LAL) ratio against shape-velocity factor k_{sv}. Box shows median value and upper/lower quartiles, whiskers show maximum and minimum values, outliers larger than 1.5 of the interquartile range are shown as red crosses. The SAL against LAL plot was shown in Figure C3. The short names of coccoliths can be found in Table 2.
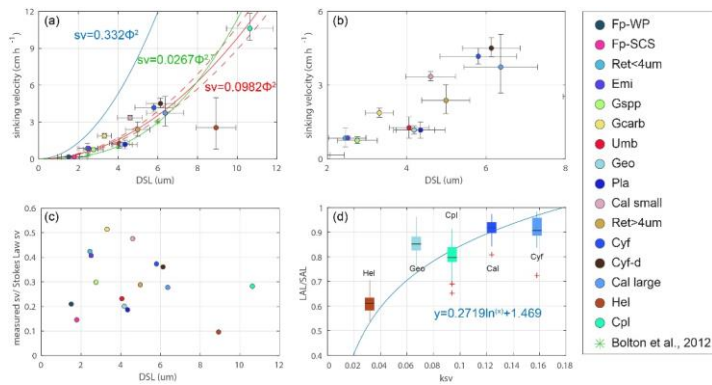
343 **Figure 7.** The selection of separation velocities: the sinking velocities of three main coccolith species

344 in sample from core KX21-2 were calculated by the length distribution and velocity factors in Table 2.

345 The yellow dots represent sinking velocities of coccoliths with mean length. The edge of boxes show

346 the sinking velocities of coccolith within one standard deviation of length ($\pm 1\sigma$) and the whiskers

347 mark the sinking velocities of coccolith within two standard deviation of length ($\pm 2\sigma$).
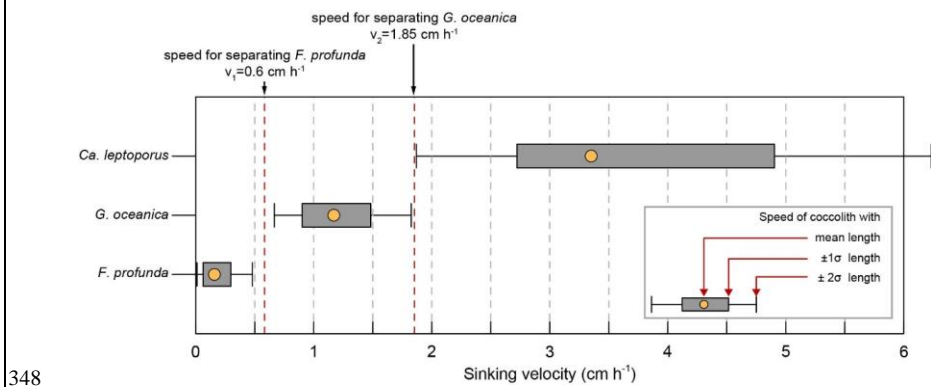
348

References

Bach, L.T., Riebesell, U., Sett, S., Febiri, S., Rzepka, P., Schulz, K.G., 2012. An approach for particle sinking velocity measurements in the 3-400 mum size range and considerations on the effect of temperature on sinking rates. Mar Biol 159, 1853-1864, doi:10.1007/s00227-012-1945-2.

Barnea, E., Mizrahi, J., 1973. A generalized approach to the fluid dynamics of particulate systems: Part 1. General correlation for fluidization and sedimentation in solid multiparticle systems. The Chemical Engineering Journal 5, 171-189, doi:10.1016/0300-9467(73)80008-5.

Baumann, K.-H., 2004. Importance of size measurements for coccolith carbonate flux estimates. Micropaleontology, 35-43.

Beaufort, L., Lancelot, Y., Camberlin, P., Cayre, O., Vincent, E., Bassinot, F., Labeyrie, L., 1997. Insolation cycles as a major control of equatorial Indian Ocean primary production. Science 278, 1451-1454, doi:10.1126/science.278.5342.1451.

Beltran, C., de Rafélis, M., Minoletti, F., Renard, M., Sicre, M.A., Ezat, U., 2007. Coccolith $\delta^{18}O$ and alkenone records in middle Pliocene orbitally controlled deposits: High-frequency temperature and salinity variations of sea surface water. Geochemistry, Geophysics, Geosystems 8, Q05003, doi:10.1029/2006GC001483.

Bolton, C.T., Hernandez-Sanchez, M.T., Fuertes, M.A., Gonzalez-Lemos, S., Abrevaya, L., Mendez-Vicente, A., Flores, J.A., Probert, I., Giosan, L., Johnson, J., Stoll, H.M., 2016. Decrease in coccolithophore calcification and CO2 since the middle Miocene. Nat Commun 7, 10284, doi:10.1038/ncomms10284.

Bolton, C.T., Stoll, H.M., 2013. Late Miocene threshold response of marine algae to carbon dioxide limitation. Nature 500, 558-562, doi:10.1038/nature12448.

Bolton, C.T., Stoll, H.M., Mendez-Vicente, A., 2012. Vital effects in coccolith calcite: Cenozoic climate-pCO2drove the diversity of carbon acquisition strategies in coccolithophores, Paleoceanography 27, doi:10.1029/2012pa002339.

Bordiga, M., Bartol, M., Henderiks, J., 2015. Absolute nannofossil abundance estimates: Quantifying the pros and cons of different techniques. Revue de micropaléontologie 58,

378   155-165 doi:10.1016/j.revmic.2015.05.002.

379 Candelier, Y., Minoletti, F., Probert, I., Hermoso, M., 2013. Temperature dependence of
380   oxygen isotope fractionation in coccolith calcite: A culture and core top calibration of the
381   genus Calcidiscus. Geochimica et Cosmochimica Acta 100, 264-281,
382   doi:10.1016/j.gca.2012.09.040.

383 Hermoso, M., Candelier, Y., Browning, T.J., Minoletti, F., 2015. Environmental control of the
384   isotopic composition of subfossil coccolith calcite: Are laboratory culture data transferable
385   to the natural environment? GeoResJ 7, 35-42, doi:10.1016/j.grj.2015.05.002.

386 Hermoso, M., Chan, I.Z.X., McClelland, H.L.O., Heureux, A.M.C., Rickaby, R.E.M., 2016.
387   Vanishing coccolith vital effects with alleviated carbon limitation. Biogeosciences 13,
388   301-312, doi:10.5194/bg-13-301-2016.

389 Jin, X., Liu, C., Poulton, A.J., Dai, M., Guo, X., 2016. Coccolithophore responses to
390   environmental variability in the South China Sea: species composition and calcite content.
391   Biogeosciences 13, 4843-4861, doi: 10.5194/bg-13-4843-2016.

392 Kell, G.S., 1975. Density, thermal expansivity, and compressibility of liquid water from 0. deg.
393   to 150. deg.. correlations and tables for atmospheric pressure and saturation reviewed and
394   expressed on 1968 temperature scale. Journal of Chemical and Engineering Data 20, 97-
395   105.

396 Kestin, J., Sokolov, M., Wakeham, W.A., 1978. Viscosity of liquid water in the range −8 °C to
397   150 °C. Journal of Physical and Chemical Reference Data 7, 941-948.

398 Koch, C., Young, J., 2007. A simple weighing and dilution technique for determining absolute
399   abundances of coccoliths from sediment samples. J. Nannoplankton Res.

400 McClelland, H.L., Bruggeman, J., Hermoso, M., Rickaby, R.E., 2017. The origin of carbon
401   isotope vital effects in coccolith calcite. Nat Commun 8, 14511,
402   doi:10.1038/ncomms14511.

403 McClelland, H.L., Barbarin, N., Beaufort, L., Hermoso, M., Ferretti, P., Greaves, M., Rickaby,
404   R.E.M., 2016. Calcification response of a key phytoplankton family to millennial-scale
405   environmental change. Scientific Reports 6, 34263, doi: 10.1038/srep34263.

406 McNown, John S., and Jamil Malaika. "Effects of particle shape on settling velocity at low

407   Reynolds numbers." Eos, Transactions American Geophysical Union 31.1 (1950): 74-82.

408   Miklasz, K.A., Denny, M.W., 2010. Diatom sinkings speeds: Improved predictions and insight

409   from a modified Stokes' law. Limnology and Oceanography 55, 2513-2525,

410   doi:10.4319/lo.2010.55.6.2513.

411   Minoletti, F., Hermoso, M., Gressier, V., ~~2008~~2009. Separation of sedimentary micron-sized

412   particles for palaeoceanography and calcareous nannoplankton biogeochemistry. Nat.

413   Protocols 4, 14-24, doi:10.1038/nprot.2008.200.

414   Paull, C.K., Thierstein, H.R., 1987. Stable isotopic fractionation among particles in Quaternary

415   coccolith-sized   deep-sea   sediments.   Paleoceanography   2,   423-429,

416   doi:10.1029/PA002i004p00423.

417   Edwards,   A.R.,   1963.   A   preparation   technique   for   calcareous   nannoplankton.

418   Micropaleontology 9, 103-104.

419   Richardson, J., Zaki, W., 1954. The sedimentation of a suspension of uniform spheres under

420   conditions of viscous flow. Chemical Engineering Science 3, 65-73.

421   Rickaby, R.E.M., Henderiks, J., Young, J.N., 2010. Perturbing phytoplankton: response and

422   isotopic fractionation with changing carbonate chemistry in two coccolithophore species.

423   Clim. Past 6, 771-785, doi:10.5194/cp-6-771-2010.

424   Rousselle, G., Beltran, C., Sicre, M.-A., Raffi, I., De Rafélis, M., 2013. Changes in sea-surface

425   conditions in the Equatorial Pacific during the middle Miocene–Pliocene as inferred from

426   coccolith   geochemistry.   Earth   and   Planetary   Science   Letters   361,   412-421,

427   doi:10.1016/j.epsl.2012.11.003.

428   Sprengel, C., Baumann, K.-H., Henderiks, J., Henrich, R., Neuer, S., 2002. Modern

429   coccolithophore and carbonate sedimentation along a productivity gradient in the Canary

430   Islands region: seasonal export production and surface accumulation rates. Deep Sea

431   Research Part II: Topical Studies in Oceanography 49, 3577-3598 doi: 10.1016/S0967-

432   0645(02)00099-1.

433   Stoll, H.M., 2005. Limited range of interspecific vital effects in coccolith stable isotopic records

434   during   the   Paleocene-Eocene   thermal   maximum.   Paleoceanography   20,

435   doi:10.1029/2004pa001046.

436 Stoll, H.M., Rosenthal, Y., Falkowski, P., 2002. Climate proxies from Sr/Ca of coccolith calcite:

437 calibrations from continuous culture of Emiliania huxleyi. Geochimica et Cosmochimica

438 Acta 66, 927-936, doi:10.1016/S0016-7037(01)00836-5.

439 Stoll, H.M., Ziveri, P., 2002. Separation of monospecific and restricted coccolith assemblages

440 from sediments using differential settling velocity. Marine Micropaleontology 46, 209-

441 221, doi: 10.1016/S0377-8398(02)00040-3.

442 ~~Tremblin, M., Hermoso, M., Minoletti, F., 2016. Equatorial heat accumulation as a long-term~~

443 ~~trigger of permanent Antarctic ice sheets during the Cenozoic. Proceedings of the National~~

444 ~~Academy of Sciences 113, 11782-11787 doi: 10.1073/pnas.1608100113.~~

445 Xie, H-Y., and D-W. Zhang. "Stokes shape factor and its application in the measurement of

446 sphericity of non-spherical particles." Powder Technology 114.1 (2001): 102-105 doi:

447 10.1016/S0032-5910(00)00269-2.

448 Young, J.R., Ziveri, P., 2000. Calculation of coccolith volume and it use in calibration of

449 carbonate flux estimates. Deep sea research Part II: Topical studies in oceanography 47,

450 1679-1700, doi:10.1016/S0967-0645(00)00003-5.

451 Zhang, H., Liu, C., Jin, X., Shi, J., Zhao, S., Jian, Z., 2016. Dynamics of primary productivity

452 in the northern South China Sea over the past 24,000 years. Geochemistry, Geophysics,

453 Geosystems 17, 4878-4891, doi:10.1002/2016GC006602 .

454 Ziveri, P., Stoll, H., Probert, I., Klaas, C., Geisen, M., Ganssen, G., Young, J., 2003. Stable

455 isotope 'vital effects' in coccolith calcite. Earth and Planetary Science Letters 210, 137-

456 149, doi:10.1016/S0012-821X(03)00101-8.

Appendix A. Sample selections

Table A1. Sample selections

| Measured coccolith	abb.	Region	Core	Section	Epoch	Age model ref.
F. profunda	Fp-SCS	SCS	MD12-3428	0-1 cm	Holocene	Zhang et al., 2016
F. profunda	Fp-WP	W.P.	KX21-2	2-4 cm	Holocene	Liang et al., 2016
E. huxleyi	Emi	SCS	MD12-3428	0-1 cm	Holocene	Zhang et al., 2016
Gephyocapsa spp.	Gspp	W.P.	ODP 807A	1H 5W 102-104	Pleistocene	Jin et al., 2010
G. oceanica	Geo	W.P.	KX21-2	2-4 cm	Holocene	Liang et al., 2016
G. caribbeanica	Gcarb	N.A.	IODP 1304B	7H 5W 69-70	Pleistocene	Channell et al., 2010
small *Reticulofenestra*	Ret<4	SCS	IODP 1433B	28R 2W 30-34	Miocene	Li et al., 2013
large *Reticulofenestra*	Ret>4	SCS	IODP 1433B	28R 2W 30-34	Miocene	Li et al., 2013
Cyclicargolithus floridanus	Cyf	SCS	IODP 1435A	6R 3W 25-29	Oligocene	Li et al., 2013
Cyclicargolithus floridanus	Cyf-d	SCS	IODP 1435A	8R 1W 27-31	Oligocene	Li et al., 2013
Umbilicosphaera sibogae	Umb	W.P.	ODP 807A	3H 5W 92-94	Pleistocene	Jin et al., 2010
Pseudoemiliania lacunosa	Pla	W.P.	ODP 807A	3H 5W 92-94	Pleistocene	Jin et al., 2010
Helicosphaera carteri	Hel	W.P.	ODP 807A	3H 5W 92-94	Pleistocene	Jin et al., 2010
large *Calcidiscus leptoporus*	Cal large	W.P.	ODP 807A	3H 5W 92-94	Pleistocene	Jin et al., 2010
small *Calcidiscus leptoporus*	Cal small	N.A.	IODP 1304B	7H 5W 69-70	Pleistocene	Channell et al., 2010
Coccolithus pelagicus	Cpl	N.A.	IODP 1304B	7H 5W 69-70	Pleistocene	Channell et al., 2010

References:

Channell, J., Sato, T., Kanamatsu, T., Stein, R., Alvarez Zarikian, C., 2010. Expedition 303/306 synthesis: North Atlantic climate. Channell, JET, Kanamatsu, T., Sato, T., Stein, R., Alvarez Zarikian, CA, Malone, MJ, and the Expedition 303, 306.

Jin, H., Jian, Z., Cheng, X., Guo, J., 2011. Early Pleistocene formation of the asymmetric east-west pattern of upper water structure in the equatorial Pacific Ocean. Chinese Science Bulletin 56, 2251-2257.

467   Li, C.-F., Lin, J., Kulhanek, D.K., 2013. South China Sea tectonics: Opening of the South

468   China Sea and its implications for southeastAsian tectonics, climates, and deep mantle

469   processes since the late Mesozoic. IODP Sci. Prosp 349.

470   Liang, D., Liu, C., 2016. Variations and controlling factors of the coccolith weight in the

471   Western Pacific Warm Pool over the last 200 ka. Journal of Ocean University of China

472   15, 456-464.

473   Zhang, H., Liu, C., Jin, X., Shi, J., Zhao, S., Jian, Z., 2016. Dynamics of primary productivity

474   in the northern South China Sea over the past 24,000 years. Geochemistry, Geophysics,

475   Geosystems 17, 4878-4891.

476 **Appendix B. Coccolith images under circular polarized light**
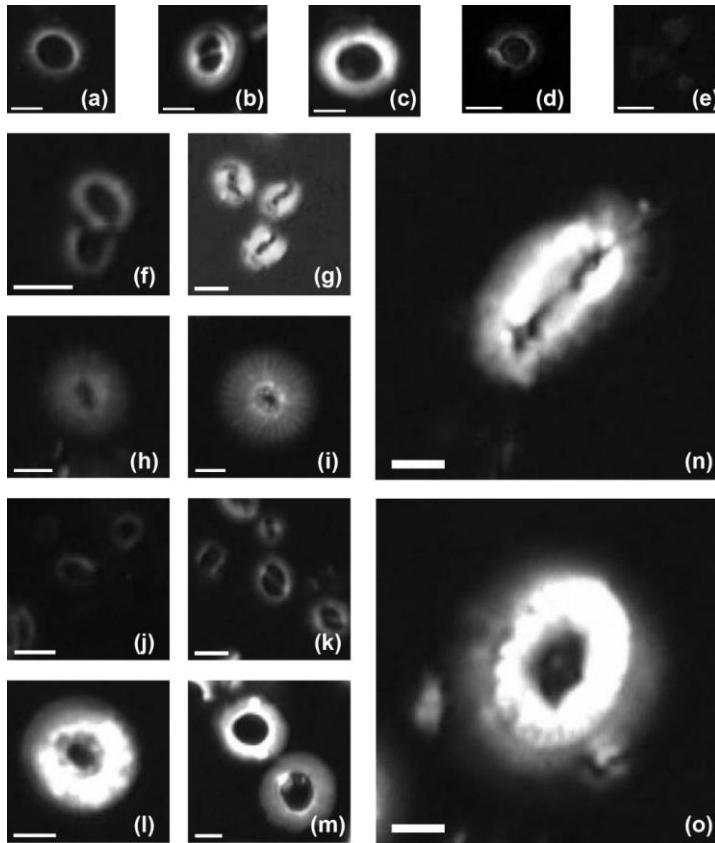
477

478 **Plate B1**. Imaged of measured coccolith in this study: (a) *Pseudoemiliania lacinosa* in the core ODP

479 807; (b) *Gephyrocapsa oceanica* in the core KX21-2; (c) *Reticulofenestra* spp. (large) in the core

480 IODP U1433B; (d) *Umbilicosphaera sibogae* in the core ODP 807; (e) *Florispharea profunda* in

481 the core KX21-2; (f) *Reticulofenestra* spp. (small) in the core IODP U1433B; (g) *Gephyrocapsa*

482 *caribbeanica* in the core IODP U1304B; (h) small *Calcidiscus leptopo~~urr~~rus* in the core IODP

483 U1304B; (i) large *Calcidiscus ~~leptopours~~ leptoporus* in the core ODP 807A; (j) *Emiliania huxleyi*

484 in the surface sediment in the South China Sea; (k) *Gephyrocapsa* spp. in the core ODP 807; (l)

485 *Cyclicargolithus floridanus* in the core IODP U1435A and (m) dissolved *Cyclicargolithus*

486 *floridanus* in the same core; (n) *Helicosphaera carteri* in the core ODP 807A; (o) *Coccolithus*

487 *pelagicus* in the core IODP U1304B. White bars represent a length of 2 μm.

26

Formatted: Font: Italic

488 **Appendix C. The length distribution of coccoliths**

489 To measure the distal shield length of coccoliths, pictures were taken at a magnification of 1250x

490 under circular polarized light. The coccolith lengths were measured by using the image analysis

491 software, ImageJ. More than 5 pictures were taken and more than 50 (usually more than 100)

492 coccolith specimens were measured. The length distributions of coccoliths measured in our

493 experiments were shown in the Figure C1.
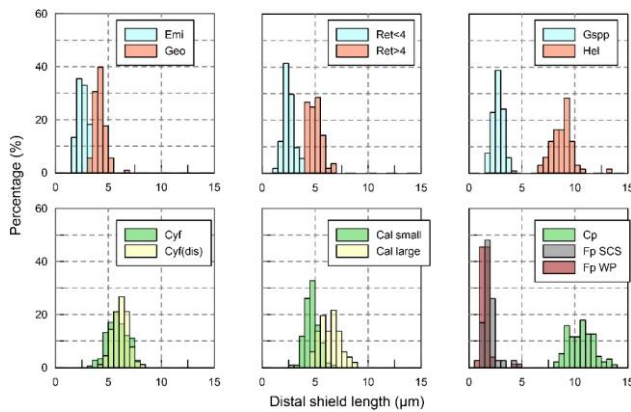
494

495 **Figure C1**. Size distribution of coccolith measured in the present study. The shorten names of coccolith

496 follow Table A1.

497 The classification of coccoliths by length was supported by mixture analysis in PAST (Hammer et

498 al., 2001), such as *Reticulofenestra* spp. and *Gephyrocapsa* spp. *Reticulofenestra* spp. in the

499 Miocene were classified into two groups, Ret. (<4 μm) and Ret. (>4 μm). The traditional

500 classification of *Reticulofenestra* spp. is <3 μm, 3-5 μm and 5-7 μm didn't pass the normal

501 distribution test. Hence, in this study the *Reticulofenestra* spp. are divided at 4 μm (Figure C2).

502 *Gephyrocapsa* spp. were classified by the shape of coccoliths into small *Gephyrocapsa* (central area

503 opening and length <3.5 μm), *G. oceanica* (central area opening and length >3.5μm) and *G.*

504 *caribbeanica* (closed central area) by the length and central area.

27

505
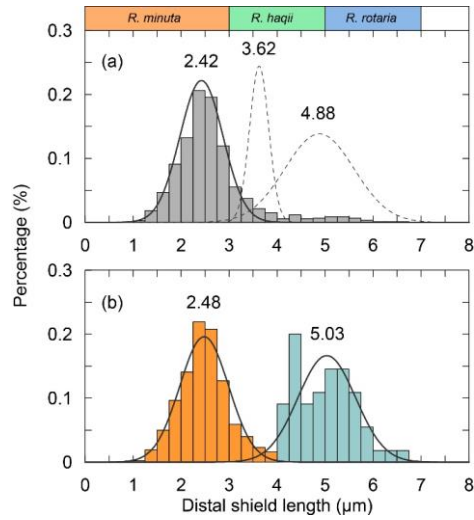
Figure C2. The classical classification of *Reticulofenestra* spp. (a) and the classification used in our study (b). The curves represent the normal distribution fits of different coccolith groups and the dish curve marks that the goodness of fit is below 0.2.

509
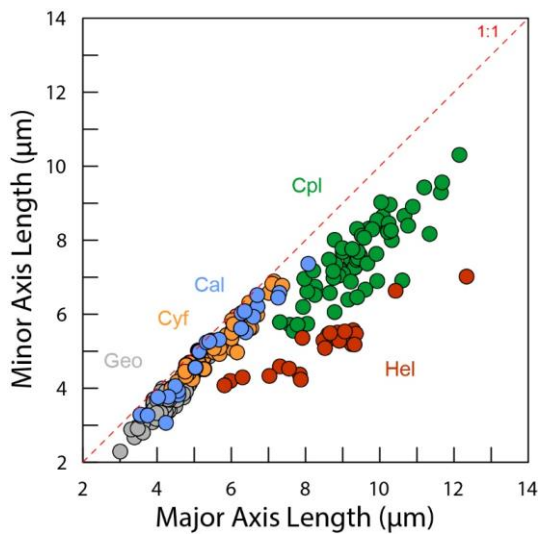
Figure C3. The short axis and long axis length distribution of coccoliths in Figure 6d.

Reference.

512   Hammer, Ø., Harper, D., Ryan, P., 2001. Paleontological Statistics Software: Package for

513   Education and Data Analysis. Palaeontologia Electronica.

Formatted: English (United States)

Appendix D. Coccolith movement in gravity settling

In this part, the derivation of equation will be explained in detail including proofs of several assumptions mentioned in the methods part.

When the well mixed sediment begins to sink, the decrease of coccoliths number in the upper suspension (N_u) can be described as following equation:

$$\frac{dN_u}{dT} = -\frac{N_{u(t=0)}}{D} \times v \tag{D-1}$$

where the D is the length of upper suspension and $N_{u(t=0)}$ /D is the initial number of coccolith in cross-section with a unit thickness, v is the sinking velocity of coccolith.

Do integration for the equation D-1, we can get the variation of coccolith number in the upper column over time:

$$N_u = N_{u(t=0)} - \frac{N_{u(t=0)}}{D} \times v \times T \tag{D-2}$$

where T is settling time. After a period of time (T), we pump out the upper suspension. Here we define the number of coccoliths in the upper supernatant dividing the total coccoliths number in the tube (N_t) as separation ratio (R), which represents the percentage of total coccoliths removed in one separation. This parameter is important and will be repeatedly mentioned in the following part. R can be expressed by

$$R = \frac{Nu}{Nt} \tag{D-3}$$

Assuming all coccoliths are uniformly distributed in the suspension at the beginning of settling, $N_{u(t=0)}$ has relationship with N_t as follow:

$$\frac{Nu(t=0)}{Nt} = \frac{V_1}{V_1 + V_2} \tag{D-4}$$

where V_1 is the volume of upper suspensions and V_2 is the volume of lower suspensions.

Combining the equation D-1, D-2, D-3 and D-4, we obtain the relationship between separation ratio, R, and sinking velocity, v, as follow:

$$R = \frac{N_u}{N_t} = \frac{N_{u(t=0)} - \frac{N_{u(t=0)}}{D} \times v \times T}{N_t} = \frac{V_1 - \frac{V_1}{D} \times v \times T}{V_1 + V_2} \tag{D-5}$$

If we plot the R and T on a figure, the slope of the line is a function of V_1, V_2, D and v. Since the V_1, V_2, D are known parameters, we say the slope of R-T is a function of v, which is exactly what we want.

542 Comparison tubes used in our experiments have the same V_1 and V_2 but different D. Other vessels

543 used in other experiments have different V_1, V_2 and D. So we should adjust the raw separation ratio

544 to calibrated separation ratio (R_{cal}), which represents the separation ratio made in a standard vessel

545 with V_{1std}=15 ml, V_{2std}=10 ml and D_{std}=6 cm. This step can be described by equation ~~2~~D-6:

546
$$RR_{cal}\text{cal} = \frac{[R\times(V_1\cancel{V1}+V_1\cancel{V2})-V_1\cancel{V1}]\times D\times V_{1std}\cancel{15}}{(D_{std}\cancel{6}\times V_1\cancel{V1}+V_{1std}\cancel{15})\times(V_{1std}+V_{2std})\cancel{25}} \qquad (D\text{-}6)$$

547 After calibrated, the slope of R_{cal}-T (k) has relationship with ~~sv~~ v as following equation:

548
$$svv = -\frac{D_{std}\times(V_{1std}+V_{2std})}{V_{1std}}\cancel{10}\times k = -10\times k \qquad (D\text{-}7)$$

549 where k is the slope of R_{cal} against T from regression and other parameters are as described above.

550 Hence, the sinking velocity of different coccoliths can be achieved by measuring the variations of

551 R_{cal} over time.

552 The coccoliths' lengths in the sediment have some varations. So what we measured is actually the

553 bulk settling velocity of whole coccolith population. We also offer a test for the assumption that the

554 average sinking velocity of all coccoliths can be treated as the sinking velocity of coccoliths with

555 the average length. Here we used the data of *G. oceanica*. A normal distribution was fitted to the

556 measured length distribution (Figure D1-a). We generated 100000 coccolith following the normal

557 distribution and let these coccolith evenly distributing in the comparison tube at the initial and then

558 set them sinking without collisions with each other. ~~And then we simulate a normal distribution~~

559 ~~situation of coccoliths in the vessel.~~ The sinking velocities of different size coccoliths were

560 calculated by the ~~cubic~~ velocity-shape parameter '~~b~~k_v' as described in discussion part. We modeled

561 the coccoliths sinking process and computed the separation ratio (red dash line in Figure D1-b),

562 coccolith length (red dash line in Figure D1-c) and instant sinking velocities (orange dots in Figure

563 D1-d) at different time sections.
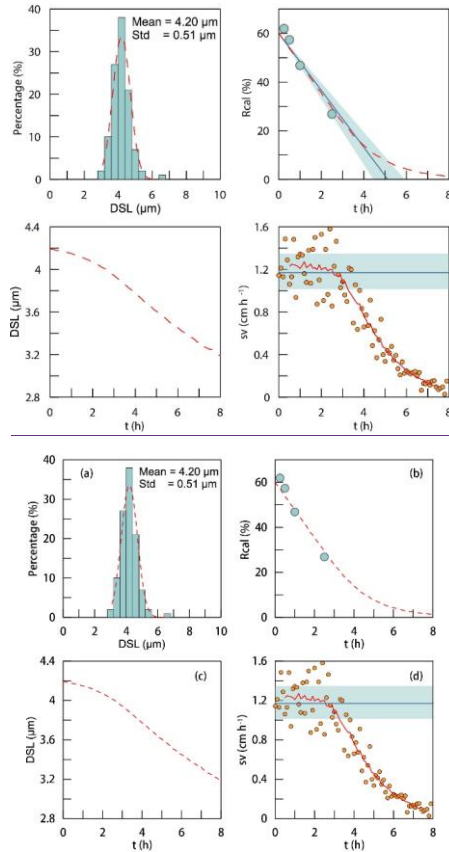
564

565

566 **Figure D1**. The simulations of coccoliths settling with different lengths: (a) the length distribution of

567 coccoliths. The green bars represent measured data and red dash line represents the best fit for normal

568 distribution. (b) The calibrated separation ratio: the green dots are measured data in our settling

569 experiments, the blue line and shade area represent the calculated sinking velocity based on R_{cal}

570 measurement and the red dash line represents results obtained from ~~Monte Carlo~~ simulations. (c) The

571 average length of removed coccolith in simulations; (d) the modeling sinking velocities of coccoliths:

572 the orange dots are instant sinking velocity calculated from derivation of R_{cal}, the red dash line is

573 weighted average for the instant sinking velocity. Blue line represents the average sinking velocity we

574 measured and the green shade area represents 95% confidence level of the measured velocity.

575 For *G. oceanica* experiments, the instant sinking velocity would not change significantly until

576 settling for more 3 hours. That means for all R_{cal} larger than 15% are safe for liner regressions. The

577 minimum safe number of R_{cal} will descend with the drop of dispersion degree of coccolith length

578 distribution. Hence our assumption for average sinking velocity and the use of liner regression are

579 proved to be reasonable.

Appendix E. Statistical and error analyses

The errors of measured separation ratio (R) and calculated sinking velocity (~~sv~~v) are mainly caused by counting coccolith, the error of which fellows the Poisson distribution. To detect the influence of counting number on the result error, the error of separation ratio was simulated by 5000 times Monte Carlo calculations with assumptions that 'V_1:V_2=15:10' and 'n_1=n_2' (Figure E1). The result shows that the number of coccolith counted in the upper column draws more influence on the relative error ($|R-R_{95CL}|/R$). That means more coccolith in the upper suspension should be counted to make results more accurate. The slope of R_{cal}-T was calculated by liner fitting with the intercept fixed on $V_1/(V_1+V_2)$. The input R_{cal} were generated from measured values considering the error of coccolith counting. The ~~error of sinking velocity~~ regressions of R_{cal}-T ~~was also~~were repeated ~~calculated~~ by 5000 times ~~Monte Carlo simulations~~regressions in the software Matlab and the error of sinking velocity, v, was source from the distribution slope of R_{cal}-T in Monte Carlo process. ~~-~~
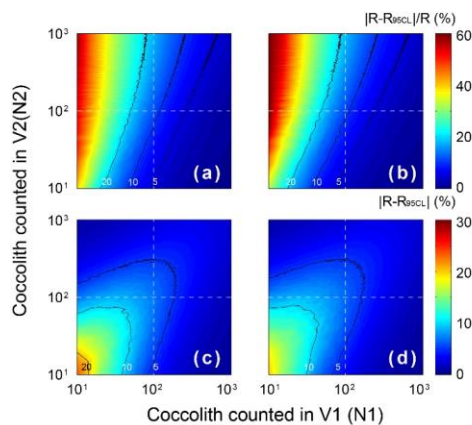
Figure E1. The error distribution with different N_1 and N_2 (ranging from 1 to 1000) simulated 5000 times by the Matlab with assumptions that the error distributions of N_1 and N_2 fellow Poisson distribution. The calculation of R follows equation 2-5, and here we assume numbers of FOV are equal (n_1=n_2). Counter lines mark values equal to 5, 10 and 20. (a) and (c) represent the lower 95% confidence level and (b) and (d) represent upper 95% confidence level. (a) and (b) the relative error of R and (c) and (d) represent the absolute error of R.